

A flow cell simulating a subsurface rock fracture for investigations of groundwater-derived biofilms

Matthew Starek,¹ Konstantin I. Kolev,² Laura Berthiaume,¹ C. William Yeung,¹
Brent E. Sleep,² Gideon M. Wolfaardt,¹ Martina Hausner^{1*}

¹Department of Chemistry and Biology, Ryerson University, Toronto, Ontario, Canada.

²Department of Civil Engineering, University of Toronto, Toronto, Ontario, Canada

Summary. Laboratory scale continuous-flow-through chambers (flow cells) facilitate the observation of microbes in a controlled, fully hydrated environment, although these systems often do not simulate the environmental conditions under which microorganisms are found. We developed a flow cell that mimics a subsurface groundwater-saturated rock fracture and is amenable to confocal laser scanning microscopy while allowing for the simple removal of the attached biomass. This flow cell was used to investigate the effect of toluene, a representative contaminant for non-aqueous phase liquids, on groundwater-derived biofilms. Reduced average biofilm biomass and thickness, and diminished diversity of amplifiable 16S rRNA sequences were observed for biofilms that developed in the presence of toluene, compared to the biofilms grown in the absence of toluene. The flow cell also allowed the detection of fluorescent protein-labelled cells. [Int Microbiol 2011; 14(3):163-171]

Keywords: *Pseudomonas putida* · biofilms · flow cells · groundwater · rock fractures · confocal microscopy

Introduction

It is widely accepted that microbes in nature tend to exist in biofilms—aggregates of cells and their extracellular substances—as opposed to a singular, planktonic existence [8]. A key aspect in the study of biofilms is the ability to perform non-invasive analyses on fully hydrated biofilms, in order to preserve their physical characteristics, as well as the spatial relationships of cells within biofilm communities. This is

especially relevant when observing biofilms in flow systems, as perturbations in the surrounding aquatic environment (or furthermore, total removal of a biofilm from its innate aquatic environment) may cause significant changes in biofilm structure and function.

The non-invasive observation of biofilms can be achieved by using flow cells, (i.e., laboratory-scale continuous flow-through chambers), which are amenable to microscopic investigation. Confocal laser scanning microscopy (CLSM) is a non-invasive technique that has been used to study both the composition and spatial arrangement of microbial populations within a biofilm [25,27] and the three dimensional architecture of the biofilm [33]. CLSM has also been used to investigate plasmid transfer in biofilms using fluorescent proteins such as green fluorescent protein (GFP) and red fluorescent protein (DsRed) [4–7,12,33,42].

*Corresponding author: M. Hausner
Department of Chemistry and Biology
Ryerson University
350 Victoria Street
Toronto, ON, Canada, M5B 2K3
Tel. +1-4169795000, ext 6553. Fax +1-4169795044
Email: martina.hausner@ryerson.ca

According to Pamp et al. [34], flow cell technology in combination with CLSM is “the gold standard in biofilm research” because it allows for observations of developmental processes in biofilms (in combination with fluorescent genetic tags), spatial organization and composition of laboratory grown biofilms in real time under continuous, non-invasive and fully hydrated conditions at the single cell level [34].

Flow cells of varying design have been employed for a variety of research purposes. These applications include the growth rate of microbes in a particular region of a biofilm [11], the spatial orientation of biofilm microbes in biofilms exposed to xenobiotics [14,48], the impact of nutrient sources on biofilm morphology [29], the effect of biofilm growth on bulk flow and solute transport [20], the influence of hydrodynamic conditions on biofilm development [43], gravimetric, optical and electrochemical investigations of microbial biofilm formation in aqueous systems [10], analysis of the transfer of plasmids between biofilm microbes [1,12,18,50], and investigations of microbial responses to environmental gradients [46]. The channels in which biofilms develop within flow chambers can be as small as 3 mm × 42 mm [48] or as large as 21 cm × 28 cm [20]; however, most flow cell channels used are closer to 3 mm × 42 mm [48].

Biofilms are ubiquitous in the environment and play an important role in a plethora of processes, including biofouling, transport processes, nutrient cycling and contaminant degradation. Many xenobiotics become adsorbed to biofilms [9,47], where they exert selective pressure on attached microbial communities resulting in the adaptation of microorganisms to the contaminant and their potential degradation. Microbial degradation is of great importance in groundwater environments. Many aquifers are situated in fractured rocks and are vulnerable to contamination from non-aqueous phase liquids (NAPL) such as hydrocarbons and chlorinated solvents. In geographical areas that rely on groundwater as a source of potable water, NAPL contamination of groundwater seriously compromises a safe and satisfactory supply of drinking water [36]. The potential of bioremediation to prevent the spreading of contamination in subsurface soils has been widely accepted. Biologically enhanced dissolution of residual source zones of NAPL in soils has also been the subject of significant interest as a potential remediation technology [38]. However, there are few studies on biodegradation processes in fractured rocks [20]. As the microbial activity in fractured rocks will be primarily associated with biofilms, elucidation of the role of biofilm processes in fractured rocks in the presence of NAPL is paramount.

The main objective of this study was to design, optimise and test a microscopy-amenable laboratory-scale flow cell that would simulate the flow of groundwater through a rock fracture aperture. This flow cell utilized a rock (shale) wafer as an attachment surface for the growth of biofilms and was employed for analysing architecture of groundwater-derived biofilms exposed to toluene—a model NAPL groundwater contaminant. Biofilms associated with the rock attachment surface could be collected for subsequent DNA extraction and fingerprinting of biofilm microbial communities. This flow-through system was subsequently used to evaluate the possibility of detecting fluorescent-protein-labelled strains, such as those of interest in bioaugmentation studies utilising the transfer of plasmids encoding catabolic genes [3–7, 32,42].

Materials and methods

Flow cell construction and other apparatus. Flow cells were constructed with the goal of simulating a model rock-fracture aperture (Fig. 1A and 1B). Teflon blocks were used for flow cell construction (outer dimensions: 2.5 cm height, 5 cm width, 7.5 cm length; inner dimensions: 2.5 cm height, 3.25 cm width, 5 cm length) (Fig. 1A). Gutters were milled at both ends of the Teflon block in the vertical plane using a 3-mm end mill piece and a Sherline model 5400 mill (Sherline, Vista, CA, USA) (Fig. 1A). Holes were drilled in both ends in the horizontal plane using a 3.175 mm drill bit and subsequently threaded. Swagelok brass straight male tube connectors (3.175 mm national pipe thread, tapered thread) were inserted into the threaded holes. Shale was used as a rock surface for the flow cells (2 cm height, 2.5 cm width, and 5 cm length). The wafer of shale was secured in the opening of the Teflon block using a two-part epoxy glue (Plastic steel putty [A] #10110, ITW, Devcon, Danvers, MA, USA). A cover slip (60 mm × 35 mm, Electron Microscopy Sciences, Ft. Washington, PA, USA) was secured over the rock wafer with solvent-resistant liquid viton (Pelseal, Newtown, PA, #2077) in order to prevent the volatilisation of toluene (Fig. 1B). Cover slips were used to allow for non-invasive examination of biofilms on the rock wafer surface by confocal microscopy (Fig. 1B). The complete experimental system set up is illustrated in Fig. 1C. Microorganisms were introduced into the flow cell through a Mininert valve (3.175 mm; Sigma-Aldrich Canada Ltd., Oakville, ON, Canada) in a Swagelok female branch tee (3.175 mm) (Fig. 1C; part 4). Teflon tubing segments were used to connect the branch tee and the straight tube connector and to join the flow cell to the effluent receptacle (Fig. 1C; part 6). A bubble trap (Fig. 1C; part 3) was positioned between the peristaltic pump (Fig. 1C; part 2) and the Swagelok brass female branch tee (Fig. 1C; part 4). Silicon tubing was used to connect the bubble trap with the flow cell. The bubble trap consisted of a 10 ml syringe, a silicon tubing inlet positioned near the top of the syringe and a silicon tubing outlet positioned near the bottom of the syringe. A multi-channel peristaltic pump (Watson-Marlow model 205S, Wilmington, MA) was used to create flow. The flow rate was set to 0.5 rpm, which corresponded to a volumetric flow rate of 3.2 ml/h.

Strains, inoculum, and culture conditions. Tryptic soy broth (TSB) (EMD, Brampton, ON) was used for all flow cell experiments.

biofilm architecture. A second set was used for DNA-based investigations of the effect of toluene on microbial diversity. Finally, two additional flow cells were used to evaluate the detection of GFP and DsRed-labelled cells against the rock wafer background. All tubing, media and glassware were autoclaved before use at 121°C for 15 min. Upon assembly, 2% sodium hypochlorite solution (v/v) was pumped through the system for 3 h. Autoclaved distilled water was then pumped through the system for 24 h. Next, 1.0% TSB was pumped through the system for 3 h to condition the attachment surface. The flow cell was inoculated with 1 ml of a previously prepared overnight culture of a groundwater-derived microbial inoculum, as described above. Flow was stopped for 2 h following inoculation and then resumed at 3.2 ml/h with 1.0% TSB. After 24 h of flow, 0.1% TSB was pumped into the flow cell for the remainder of the experiment in order to simulate a low-nutrient groundwater environment.

To simulate NAPL contamination, 600 µl of neat toluene was introduced into the flow cell through the Mininert valve in a Swagelok brass female branch tee (Fig. 1C; part 4). Toluene remained in the organic phase as an irregularly shaped globule of approx. 10 mm in diameter in the flow cell between the cover glass and rock surface, simulating a contaminated rock fracture.

Biofilm architecture analysis. Medium flow was stopped after 12 days of biofilm development and the biofilms were stained with 500 µl of 50 mM acridine orange (EMD, Mississauga, ON, Canada) dissolved in sterile water. The flow cells were covered with aluminum foil to avoid photo-bleaching of the acridine orange signal, and kept for 15 min before flow was resumed for 5 min to remove any unbound stain or stained planktonic cells. Flow cells were then examined with a confocal laser scanning microscope (Zeiss, LSM510, Jena, Germany). Images were obtained using a 488-nm laser and a 505- to 530-nm band-pass emission filter. A 20×/0.75 Fluor objective lens (Zeiss, Jena, Germany), with a working distance of 0.66 mm, was used together with a 2× digital zoom. Image stacks were collected at 2-µm increments.

Fifteen image stacks were analysed from toluene- and non-toluene-treated microbial cultures using the COMSTAT program [19] for the average quantification of biofilm biomass and biofilm thickness. COMSTAT is an image analysis script that runs in MATLAB (The Math Works, MA, USA). Average biofilm biomass was quantified as the volume of biomass per substratum area (µm³/µm²). Thickness was measured as the mean thickness of the biofilm (µm). A single factor analysis of variance (ANOVA) ($p = 0.05$) using Excel's data analysis tool was utilized for statistical analysis of differences in the biofilm biomass of toluene-exposed and untreated biofilms.

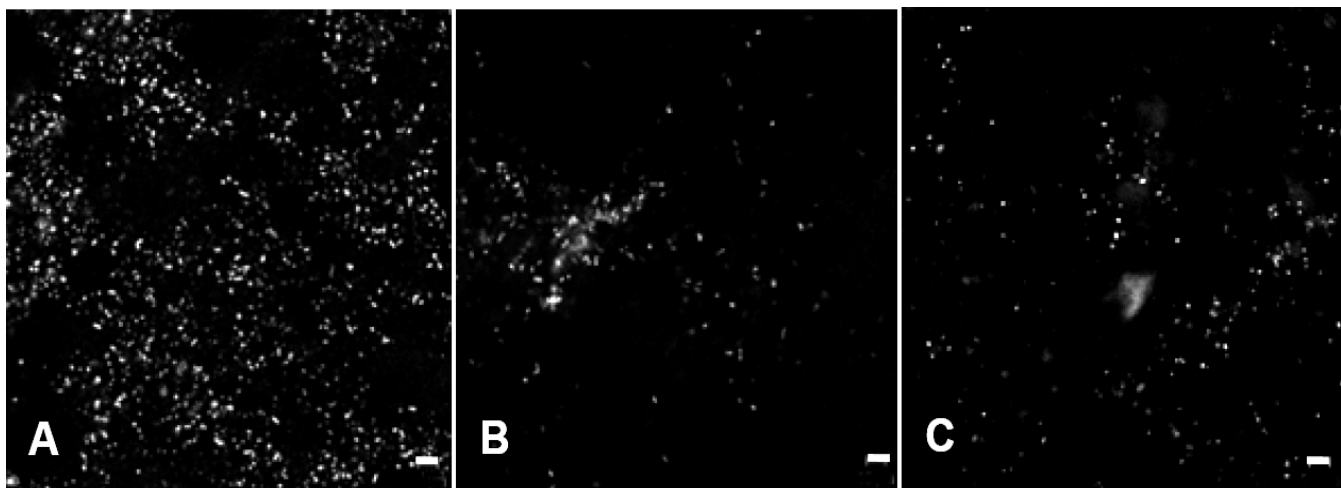
Detection of GFP or DsRed-expressing cells in the flow cell. To test the limits of detection of donor and transconjugant cells against the heterogeneous rock wafer background, cells expressing GFP or DsRed were injected into the flow cell through the inoculation port. Medium flow was stopped for 1 h, in order to facilitate the attachment of cells, and then resumed. CLSM was then used to examine the flow cells for the presence of fluorescent cells, with the detection of autofluorescence emanating from the rock wafer surface minimised using band pass emission filters. A 505- to 530-nm emission filter was used for the detection of GFP fluorescence, and a 560- to 615-nm emission filter for the detection of DsRed fluorescence. Images were taken 1 h after inoculation and subsequently every third day. The flow cell was in operation for 12 days after inoculation.

Biofilm collection and DNA extraction. Biofilm samples from the surface of the rock wafer inside the flow cell were obtained at the end of

the experiment by clamping the flow system tubing and removing the flow cell from the flow system, followed by aseptic removal of the Viton sealant. A cell scraper (#179707, Thermo Scientific, Rochester, NY, USA) was used to scrape the surface of the rock wafer and cover glass. Collected biomass was placed in saline solution and centrifuged at 5000 ×g to a pellet for DNA extraction. From each flow system, 50 ml of effluent was collected at the end of the experiment and centrifuged at 5000 ×g to a pellet for DNA extraction, performed using a GeneElute Bacterial Genomic DNA kit (#NA2110, Sigma-Aldrich, Oakville, ON, Canada).

PCR and denaturing gradient gel electrophoresis (DGGE). Primers U341F-GC (5'-CCTACGGGAGGCAGCAG-3'), which had a GC clamp attached (5'-GGCGGGCGGGGCACGGGGGGCGCGCGG GCGGGGCGGGG-3') at the 5' end [30], and U758R (5'-CTACCA GGGTATCTAATCC-3') were used to amplify a 418-bp fragment corresponding to positions 341–758 in the *Escherichia coli* 16S sequence within the variable regions V3 and V4 [35]. Primers were synthesized by The SickKids Centre for Applied Genomics (TCAG) Synthesis Facility (Toronto, ON, Canada). The 50-µl PCR reaction mixture contained 1 µl of template DNA, autoclaved distilled water, 25 pmol of both the forward and reverse primer, 10× BSA (New England BioLabs, Pickering, ON), 200 µM of each dNTP (New England BioLabs, Pickering, ON) and 2.5 units of Taq polymerase (New England BioLabs, Pickering, ON) in 1× Taq buffer (10 mM Tris-HCl pH 9.0, 50 mM KCl, 1.5 mM MgCl₂) (New England BioLabs, Pickering, ON). The PCR protocol was as follows: 96°C for 5 min and thermocycling at 94°C for 1 min; an annealing temperature of 65°C with a 1°C decrease every 1 min cycle for 20 cycles, and a 3 min elongation time at 72°C. Additional cycles (15–20) were carried out at annealing temperatures of 55°C [51]. Upon completion of the protocol, the samples were loaded into a 1% agarose gel with SYBR Safe DNA gel stain (Invitrogen, Burlington, ON), visualized using the Invitrogen Safe Imager 2.0 (Invitrogen) and quantified using a serial dilution of a 100-bp molecular weight (MW) ladder (MBI Fermentas, Amherst, NY, USA) to create a standard curve. Each sample was amplified three separate times using the same PCR protocol, to minimize PCR bias. The products were combined, cleaned using the IBI Gel/PCR DNA fragments extraction kit (IBI Scientific, Peosta, IA), and concentrated, if necessary, using a Savant DNA110 speed vacuum (Fisher Scientific Limited, Nepean, ON, Canada). Quantification was performed using the same agarose gel setup and MW ladder as mentioned previously.

The DGGE gel consisted of 8% polyacrylamide with a denaturing gradient of 30–70% (7 M urea and 40% deionized formamide were defined as 100% denaturant) and was cast using a gradient former (BioRad Laboratories, Mississauga, ON, Canada). Approximately 500 ng of the 16S rRNA gene product was loaded into each well of the DGGE gel. The gel was run in a DCode Universal Mutation Detection System (BioRad Laboratories, Mississauga, ON). Electrophoresis was carried out at a constant voltage of 80 V for 16 h at 60°C. All gels were stained for 30 min in SYBR Gold (Invitrogen, Burlington, ON) with gentle agitation followed by brief destaining in 1× TAE. The gel was imaged using a Gel Logic 1500 Imaging System (Kodak, Rochester, NY, USA) and the images then analysed using GelCompar II v6.5 (Applied Maths, Sint-Martens-Latem, Belgium) to generate dendrogram profiles. The genotypes were visually detected based on the presence or absence of bands in the different lanes. A band was defined as present if the ratio of its peak height to the total peak height in the profile was >5%. After conversion and normalisation of the gels using GelCompar, the degrees of similarity of the DNA pattern profiles were calculated using the Dice similarity coefficient [13] and dendrogram patterns were clustered by the unweighted pair group method using arithmetic average (UPGMA) groupings to generate a similarity coefficient (S_{AB}) matrix.



Int. Microbiol.

Fig. 2. Detection of GFP-expressing strain *Pseudomonas putida* SM1443::*gfp2x-pWW0::dsRed* and red fluorescent protein-expressing cells within the flow cell. DsRed-expressing transconjugants were visualized using confocal microscopy on the surface of the rock wafer in the flow cell 1 h after inoculation (A) and 12 days after inoculation (B). GFP-expressing cells were detected 4 days after inoculation on the surface of the rock wafer (C). Autofluorescence of the rock wafer was minimised by using band pass detection filters to collect both DsRed and GFP signals. Scale bar: 10 μ m.

Results and Discussion

Flow cell design and construction. The subsurface environment is characterized by low flow and large surface-to-pore volume ratios. Therefore, conventional experimental systems that do not provide comparable flow rates and surfaces for biofilm formation may introduce selection pressure for opportunistic species with little relevance in situ. The inclusion of gutters in the flow cell design ensured uniform flow of the growth medium used to support biofilm growth on the rock wafer surface (Fig. 1A,B).

Glass is the most common attachment surface that has been used in conventional flow cells [23,43], while the flow cell body may be manufactured from Teflon [M. Starek. M.Sc. Thesis], plexiglass [49] or stainless steel [18,23,31, 43,50]. For studies of subsurface microorganisms, geological material (e.g., rock or mineral wafers) that simulates the natural environment, as an attachment surface for biofilm development, is preferable to glass. Previous studies of the microbial weathering of sulphide minerals employed flow cells with polished thin sections prepared from sulphide mineral-containing rocks as microbial attachment surfaces [24]. While these flow cells provide environmental attachment surfaces for biofilm development, they are typically not closed system (a glass cover slide is not sealed to the top of the flow cell), and thus are not suitable for experiments involving volatile substances. In contrast, in the system des-

cribed here (Fig. 1C), Teflon was used for flow cell (Fig. 1B) construction, and Teflon tubing was placed between the medium reservoir and the flow cell, thus allowing the testing of volatile compounds, such as toluene, the model NAPL substrate used in this study.

Toluene, together with benzene, ethylbenzene and xylene (BTEX), are aromatic compounds characterized by a relatively low solubility in aqueous solutions. Consequently, they are often present in groundwater as NAPLs [2]. Aerobic degradation of BTEX compounds can be accomplished by microorganisms expressing either monooxygenases or dioxygenases, but other pathways have also been described [41]. The TOL plasmid pWWO [16], initially isolated from *Pseudomonas putida*-mt2 [45], contains genes that encode monooxygenases that degrade toluene/xylene [16]. In addition, the TOL plasmid pWWO encodes and constitutively expresses genes necessary for the transfer of the plasmid from host to recipient [16]. Other hosts, in addition to *Pseudomonas* strains, have been reported to successfully receive the TOL plasmid, including members of the genera *Erwinia* and *Serratia* [28]. Toluene can be also degraded in the absence of oxygen by different microorganisms, including the beta-proteobacterial species within the *Thauera* and *Azoarcus* genera [44].

Microscopic observations. The transfer of catabolic plasmids such as the TOL plasmid can be monitored with the use of fluorescent proteins, including GFP and DsRed

[4–7,32,42]. With the aid of bandpass filters it was possible to minimise rock autofluorescence, thus allowing the detection of red-fluorescing cells (transconjugant cells, Fig. 2A, 2B) and of green-fluorescing cells (donor cells, Fig. 2C) using 560–615 nm and 505–530 nm emission filters, respectively. This is of importance, as fluorescent proteins, among other uses, are employed in the study of gene transfer between bacteria [4–7,32,42]. Horizontal gene transfer (HGT) is a successful mechanism to spread plasmids harbouring genes encoding degradative enzymes in model wastewater and model soil systems, in which a lab-designed donor strain has been introduced into the model system [1, 4–7,32,42]. There is not, however, much information with respect to the transfer of degradative plasmids between bacteria in model groundwater systems [21,39] and, more specifically, in rock-fracture apertures. Therefore, the flow cell system described in this work is a useful tool with which to evaluate the feasibility of gene transfer in rock fracture aquifers [M. Starek. M.Sc. Thesis]. Transconjugant red-fluorescing cells were observed attached to the rock surface 1 h after inoculation (Fig. 2A), indicating the tendency of these groundwater bacteria to associate with and colonise solid surfaces. Furthermore, the transconjugant cells were observed for the duration of the experiment (12 d, Fig. 2B), which is evidence of subsequent biofilm formation.

Image analysis revealed that biofilms grown in the presence of toluene occupied an average biovolume of $1.1 \mu\text{m}^3$ per μm^2 footprint area, and were on average $2.6\text{-}\mu\text{m}$ thick while untreated biofilms occupied an average of $1.9 \mu\text{m}^3$ per μm^2 footprint area and were on average $7.1\text{-}\mu\text{m}$ thick. Biovolume is the biomass volume per substratum (rock surface) area and provides an estimate of biofilm biomass [19]. The thickness value reflects the spatial size of the biofilm [19]. In our study, the biovolume and thickness values obtained for toluene-exposed biofilms were significantly different from values obtained for biofilms grown in the absence of toluene, as revealed by a single-factor ANOVA analysis using a $p = 0.05$.

Effect of toluene on microbial diversity. DGGE fingerprinting of biofilm and effluent samples suggested that the differences in biofilm structure detected by confocal microscopy and image analysis were accompanied by changes in community composition. The DGGE profiles (Fig. 3) of amplified 16S rDNA fragments extracted from toluene-exposed biofilm and those from untreated biofilm differed from each other. The DGGE fingerprint of the

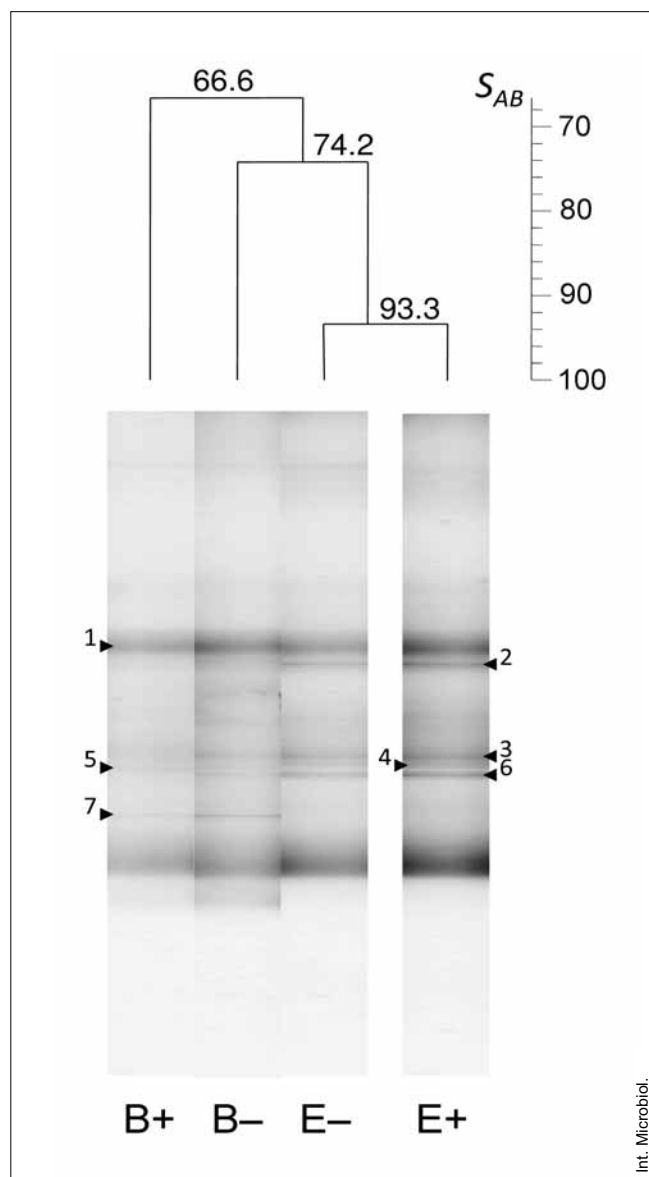


Fig. 3. Dendrogram of bacterial DGGE with cluster analysis of the banding patterns of fingerprints of toluene-exposed biofilm (B+), untreated biofilm (B-), effluent collected from the untreated biofilm (E-) and effluent collected from the toluene-treated biofilm (E+). A similarity coefficient (S_{AB}) matrix was generated using the unweighted pair group method based on arithmetic average (UPGMA) groupings.

untreated biofilm showed greater band diversity. For example, the band corresponding to band 6 in lanes B-, E-, and E+ (Fig. 3) was not detected in the toluene-exposed profile (B+). Similarly, the band corresponding to band 3 in lanes B-, E- and E+ (Fig. 3) was not detected in the toluene-exposed biofilm profile (lane B+, Fig. 3).

While three prominent bands (bands 1, 5 and 7, Fig. 3) were clearly visible in the toluene-exposed biofilm profile

(B+), only bands 1 and 7 were clearly visible in the untreated biofilm profile (B-). Band 5 was present in the untreated biofilm profile (B-) but was less intense than the corresponding band in the toluene-treated biofilm profile (B+). Two of the three bands (5 and 7, in lanes B+ and B-, Fig. 3) were not visible in the effluent profiles (lanes E- and E+), suggesting that the microorganisms corresponding to these bands were not frequently shed into the effluents. Effluent sample profiles mostly reflected the unexposed-biofilm profile, except for band 2 in lanes E- and E+ and band 4 in lanes E- and E+ (Fig. 3), which were not visible in the biofilm profiles. This could be explained either by preferential shedding of these particular species into effluents or enhanced proliferation in the effluent reservoir. Since the toluene-exposed biofilm profile differed from the unexposed-biofilm profile, the fact that the effluent profiles were highly similar suggests that the same types of microorganisms detached from both treated and untreated biofilms early in the experiment and then proliferated in the effluent vessels.

DGGE profiles from biofilm and effluent samples (Fig. 3) revealed a high similarity, with a binary association coefficient (S_{AB} value) of 93.3% for the two effluent fingerprints. The effluent profiles showed 74.2% similarity to the untreated biofilm profile. The toluene-exposed biofilm profile was the least similar to the other three profiles, with only 66.6% of the S_{AB} value.

The DGGE data indicated that no major selection of specific microorganisms occurred due to toluene exposure; however, toluene exposure led to changes in the initial microbial community, as demonstrated by a decrease in the number of bands in the toluene-exposed biofilm profile compared to the unexposed biofilm and effluent sample profiles. Similar observations were made by Hendrickx et al. [17], who investigated the dynamics of bacterial aquifer communities during contact with a toluene-contaminated plume. In that study, the richness of 16S rRNA sequences was lower in the toluene contaminated locations than in the uncontaminated locations, a finding in contrast to the observations made by Shi et al. [37], who observed similar relative abundances of *Proteobacteria* and gram-positive bacteria in fuel-contaminated and uncontaminated aquifer materials. Lee et al. [26] observed shifts in groundwater community profiles, in addition to the persistence of some members with varying levels of BTEX contamination. They noted that changes in the community profiles were a function of BTEX concentration, dissolved oxygen concentration, and carbon source. Ji et al. [22] recorded changes in the community profile of a microbial

community in BTEX-contaminated soil and an increase in *Actinobacteria* and *Bacillus* populations. They further observed bands that were unique to contaminated and uncontaminated samples. Similarly, Fahy et al. [15] observed a shift from Betaproteobacteria to Actinobacteria in response to benzene exposure.

The experimental flow cell described here offers a way to observe and evaluate biofilm architecture and composition as well as the remediation potential of microbes or mixed microbial communities. In our study, the exposure of biofilms in flow cells to toluene led to a reduction of biofilm biomass. Further, DGGE fingerprinting of PCR-amplified 16S rRNA fragments demonstrated that microbial diversity in the toluene-exposed biofilm was diminished. The flow cell system also allowed for the visualisation of GFP-tagged donor cells and DsRed-expressing transconjugant cells against the background autofluorescence associated with the rock wafer surface, a useful feature for gene transfer studies in simulated rock fracture environments.

Acknowledgements. This work was supported by a National Sciences and Engineering Council of Canada (NSERC) Discovery Program-Individual grant to MH (grant no. 355606-2008), by Ryerson University and by funding to BES from the Ontario Ministry of the Environment Best-in-Science Program. We are grateful to David Jenkins (Ryerson University) for generating the flow cell and experimental system drawings.

Competing interests. None declared.

References

1. Aspray TJ, Hansen SK, Burns RG (2005) A soil-based microbial biofilm exposed to 2,4-D: bacterial community development and establishment of conjugative plasmid pJP4. *FEMS Microbiol Ecol* 54:317-327
2. Aydin GA, Agaoglu B, Kocasoy G, Copty NK (2011) Effect of temperature on cosolvent flooding for the enhanced solubilization and mobilization of NAPLs in porous media. *J Hazard Mater* 186:636-44
3. Bathe S, Hausner M (2010) Plasmid-mediated bioaugmentation of wastewater microbial communities in a laboratory-scale bioreactor. *Methods Mol Biol* 599:185-200
4. Bathe S, Leuhn M, Ellwart JW, Wuertz S, Hausner M (2004) High phylogenetic diversity of transconjugants carrying plasmid pJP4 in an activated sludge-derived microbial community. *FEMS Microbiol Lett* 235:215-219
5. Bathe S, Mohan TVK, Wuertz S, Hausner M (2004) Bioaugmentation of a sequencing batch biofilm reactor by horizontal gene transfer. *Water Sci Technol* 49:337-344
6. Bathe S, Schwarzenbeck N, Hausner M (2005) Plasmid-mediated bioaugmentation of activated sludge bacteria in a sequencing batch moving bed reactor using pNB2. *Lett Appl Microbiol* 41:242-247

7. Bathe S, Schwarzenbeck N, Hausner M (2009) Bioaugmentation of activated sludge towards 3-chloroaniline removal with a mixed bacterial population carrying a degradative plasmid. *Bioresour Technol* 100:2902-2909
8. Battin TJ, Sloan WT, Kjelleberg S, Daims H, Head IM, Curtis TP, Eberl L (2007) Microbial landscapes: new paths to biofilm research. *Nat Rev Microbiol* 5:76-81
9. Bouwer EJ (1989) Transformation of xenobiotics in biofilms. In: Characklis WG, Wilderer PA (eds) *Structure and function of biofilms*. John Wiley, New York, NY, USA, pp 251-267
10. Bressel AJ, Schultze W, Khan W, Wolfaardt GM, Rohns HP, Irmischer R, Schoning MJ (2003) High resolution gravimetric, optical and electrochemical investigations of microbial biofilm formation in aqueous systems. *Electrochim Acta* 48:3363-3372
11. Caldwell DE, Lawrence JR (1986) Growth kinetics of *Pseudomonas fluorescens* microcolonies within the hydrodynamic boundary layers of surface microenvironments. *Microb Ecol* 12:299-312
12. Christensen BB, Sternberg C, Andersen JB, Eberl L, Moller S, Givskov M, Molin S (1998) Establishment of new genetic traits in a microbial biofilm community. *Appl Environ Microbiol* 64:2247-2255
13. Dice LR (1945) Measures of the amount of ecologic association between species. *Ecol* 26:297-302
14. Ebihara T, Bishop PL (1999) Biofilm structural forms utilized in bioremediation of organic compounds. *Water Sci Technol* 39:203-210
15. Fahy A, Bail AS, Lethbridge G, Timmis KN, McGenity TJ (2008) Isolation of alkali-tolerant benzene-degrading bacteria from a contaminated aquifer. *Lett Appl Microbiol* 47:60-66
16. Greated A, Lamberts L, Williams PA, Thomas CM (2002) Complete sequence of the IncP-9 TOL plasmid pWW0 from *Pseudomonas putida*. *Environ Microbiol* 4:856-871
17. Hendrickx B, Dejonghe W, Boëne W, Brennerova M, Cernik M, Lederer T, Bucheli-Witschel M, Bastiaens L, Verstraete W, Top EM, Diels L, Springael D (2005) Dynamics of an oligotrophic bacterial aquifer community during contact with a groundwater plume contaminated with benzene, toluene, ethylbenzene, and xylenes: an in situ mesocosm study. *Appl Environ Microbiol* 71:3815-3825
18. Hendrickx L, Hausner M, Wuertz S (2003) Natural genetic transformation in monoculture *Acinetobacter* sp. strain BD413 biofilms. *Appl Environ Microbiol* 69:1721-1727
19. Heydorn A, Nielsen AT, Hentzer M, Sternberg C, Givskov M, Ersboll BK, Molin S (2000) Quantification of biofilm structures by the novel computer program COMSTAT. *Microbiol* 146:2395-2407
20. Hill DD, Sleep BE (2002) Effects of biofilm growth on flow and transport through a glass parallel plate fracture. *J Contam Hydrol* 56:227-246
21. Jain R, Sayler G, Wilson JT, Houston LT, Pacia D (1987) Maintenance and stability of introduced genotypes in groundwater aquifer material. *Appl Environ Microbiol* 53: 996-1002
22. Ji SC, Kim D, Yoon JH, Lee CH (2007) Metagenomic analysis of BTEX-contaminated forest soil microcosm. *J Microbiol Biotechnol* 17:668-672
23. Kuehn M, Hausner M, Bungartz HJ, Wagner M, Wilderer PA, Wuertz S (1998) Automated confocal laser scanning microscopy and semiautomated image processing for analysis of biofilms. *Appl Environ Microbiol* 64:4115-4127
24. Lawrence JR, Kwong Y TJ, Swerhone GDW (1997) Colonization and weathering of natural sulfide mineral assemblages by *Thiobacillus ferrooxidans*. *Can J Microbiol* 43: 178-188
25. Lawrence JR, Neu TR (1999) Confocal laser scanning microscopy for analysis of microbial biofilms. *Meth Enzymol* 310:131-144
26. Lee EH, Kim J, Kim JY, Koo SY, Lee SD, Ko KS, Ko DC, Yum BW, Cho KS (2010) Comparison of microbial communities in petroleum-contaminated groundwater using genetic and metabolic profiles at Kyonggi-Do, South Korea. *Environ Earth Sc* 60:371-382
27. Manz W, Wendt-Potthoff K, Neu TR, Szwedzyk U, Lawrence JR (1999) Phylogenetic composition, spatial structure, and dynamics of lotic bacterial biofilms investigated by fluorescent in situ hybridization and confocal laser scanning microscopy. *Microb Ecol* 37:225-237
28. Mølbak L, Licht TR, Kvist T, Kroer N, Andersen SR (2003) Plasmid transfer from *Pseudomonas putida* to the indigenous bacteria on alfalfa sprouts: characterization, direct quantification, and in situ location of transconjugant cells. *Appl Environ Microbiol* 69:5536-5542
29. Moller S, Korber DR, Wolfaardt GM, Molin S, Caldwell DE (1997) Impact of nutrient composition on a degradative biofilm community. *Appl Environ Microbiol* 63:2432-2438
30. Muyzer G, Dewaal EC, Uitterlinden AG (1993) Profiling of complex microbial-populations by denaturing gradient gel-electrophoresis analysis of polymerase chain reaction-amplified genes-coding for 16S ribosomal RNA. *Appl Environ Microbiol* 59:695-700
31. Nanchaiah YV, Venugopalan VP, Wuertz S, Wilderer PA, Hausner M (2005) Compatibility of the green fluorescent protein and a general nucleic acid stain for quantitative description of a *Pseudomonas putida* biofilm. *J Microbiol Methods* 60:179-187
32. Nanchaiah YV, Wattiau P, Wuertz S, Bathe S, Mohan SV, Wilderer PA, Hausner M (2003) Dual labeling of *Pseudomonas putida* with fluorescent proteins for in situ monitoring of conjugal transfer of the TOL plasmid. *Appl Environ Microbiol* 69:4846-4852
33. Neu TR, Woelfl S, Lawrence JR (2004) Three-dimensional differentiation of photo-autotrophic biofilm constituents by multi-channel laser scanning microscopy (single-photon and two-photon excitation). *J Microbiol Methods* 56:161-172
34. Pamp SJ, Sternberg C, Tolker-Nielsen T (2009) Insight into the microbial multicellular lifestyle via flow-cell technology and confocal microscopy. *Cytometry A* 75:90-103
35. Rolleke S, Muyzer G, Wawer C, Wanner G, Lubitz W (1996) Identification of bacteria in a biodegraded wall painting by denaturing gradient gel electrophoresis of PCR-amplified gene fragments coding for 16S rRNA. *Appl Environ Microbiol* 62:2059-2065
36. Rubin H, Yaniv S, Spiller M, Kongeter J (2008) Parameters that control the cleanup of fractured permeable aquifers. *J Contam Hydrol* 96:128-149
37. Shi Y, Zwolinski MD, Schreiber ME, Bahr JM, Sewell GW, Hickey WJ (1999) Molecular analysis of microbial community structures in pristine and contaminated aquifers: field and laboratory microcosm experiments. *Appl Environ Microbiol* 65:2143-2150
38. Sleep BE, Seepersad DJ, Kaiguo MO, Heidorn CM, Hrapovic L, Morrill PL, McMaster L, Hood ED, Lebron C, Lollar BS, Major DW, Edwards EA (2006) Biological enhancement of tetrachloroethene dissolution and associated microbial community changes. *Environ Sci Technol* 40: 3623-3633
39. Smets BF, Morrow JB, Pinedo A (2003) Plasmid introduction in metal-stressed, subsurface-derived microcosms: plasmid fate and community response. *Appl Environ Microbiol* 69:4087-4097
40. Tolker-Nielsen T, Brinch UC, Ragas PC, Andersen JB, Jacobsen JC, Molin S (2000) Development and dynamics of *Pseudomonas* sp. biofilms. *J Bacteriol* 182:6482-6489
41. Van Agteren MH, Keuning S, Janssen DB (1998) *Handbook on biodegradation and biological treatment of hazardous organic compounds*, Kluwer Academic Publishers, London, UK

42. Venkata Mohan S, Falkentoft C, Nancharaiyah VY, Sturm BS, Wattiau P, Wilderer PA, Wuertz S, Hausner M (2009) Bioaugmentation of microbial communities in laboratory and pilot scale sequencing batch biofilm reactors using the TOL plasmid. *Bioresour Technol* 100:1746-1753
43. Venugopalan VP, Kuehn A, Hausner M, Springael D, Wilderer PA, Wuertz S (2005) Architecture of a nascent *Sphingomonas* sp. biofilm under varied hydrodynamic conditions. *Appl Environ Microbiol* 71: 2677-2686.
44. Weelink SAB, van Eekert MHA, Stams AJM (2010) Degradation of BTEX by anaerobic bacteria: physiology and application. *Rev Environ Sci Biotechnol* 9:359-385
45. Williams PA, Murray K (1974) Metabolism of benzoate and the methylbenzoates by *Pseudomonas putida* (arvilla) mt-2: evidence for existence of a TOL plasmid. *J Bacteriol* 120:416-423
46. Wolfaardt GM, Hendry MJ, Birkham T, Bressel A, Gardner MN, Sousa AJ, Korber DR, Pilaski M (2008) Microbial response to environmental gradients in a ceramic-based diffusion system. *Biotechnol Bioeng* 100: 141-149
47. Wolfaardt GM, Lawrence JR, Headley JV, Robarts RD, Caldwell DE (1994) Microbial exopolymers provide a mechanism for bioaccumulation of contaminants. *Microb Ecol* 27:279-291
48. Wolfaardt GM, Lawrence JR, Hendry MJ, Robarts RD, Caldwell DE (1993) Development of steady-state diffusion gradients for the cultivation of degradative microbial consortia. *Appl Environ Microbiol* 59: 2388-2396
49. Wolfaardt GM, Lawrence JR, Robarts RD, Caldwell SJ, Caldwell DE (1994) Multicellular organization in a degradative biofilm community. *Appl Environ Microbiol* 60:434-446
50. Wuertz S, Hendrickx L, Kuehn M, Rodenacker K, Hausner M. 2001. In situ quantification of gene transfer in biofilms. *Method Enzymol* 336: 129-143
51. Yeung CW, Lee K, Greer CW (2011) Characterization of the bacterial community structure of Sydney Tar Ponds sediment. *Can J Microbiol* 57:493-503